Do embedded volcanoclastic layers serve as potential glide planes? – An integrated analysis from the Gela Basin offshore southern Sicily

J. Kuhlmann[1], K. Huhn[1], M.J. Ikari[1]

[1]MARUM – Center for Marine Environmental Sciences and Faculty of Geosciences, University of Bremen, Leobener Str., D-28359 Bremen, Germany

Corresponding author E-Mail: jkuhlmann@marum.de

Abstract The NE portion of the Gela Basin (Strait of Sicily) shows evidence of multiple mass wasting events of predominantly translational character. In this context, recent investigations implicate volcanoclastic layers as key stratigraphic surfaces acting as preferential planes of failure. We present an integrated analysis of a representative sedimentary transition from overlying homogeneous background sedimentation of silty clay to a volcanoclastic layer. A high-resolution CT scan and three drained direct-shear laboratory experiments from a 20 cm whole-round section (~28.2 mbsf) allow the delineation of the role of this volcanoclastic layer in the framework of slope stability and failure initiation. The mechanical results indicate a general strengthening of the material with increased volcanoclastic content. Tendency for failure is expected to be highest within the silty clay due to relatively lower shear strength and strain-weakening behaviour, which promotes progressive sediment failure. In contrast with recent findings, this suggests that volcanoclastic sediment would not act as a weak layer. However, the volcanoclastic layer exhibits significant mesoporosity (i.e., fracturing) and may therefore host large volumes of fluid. Temporarily undrained conditions, for example during seismic activity, could transiently elevate fluid pressures and thus reduce the material shear strength below that of the surrounding silty clay. Such a weak layer may preferentially form along the interface of fractured volcanoclastic material and relatively impermeable silty clay, where differences in material strengths are lowest.

Keywords: MeBo, slope failure, volcanoclastic layer, shear strength, fracturing

1. Introduction

The destabilization of continental slopes in form of bedding-parallel translational slides is frequently related to discrete *weak layers* and their material properties (e.g., Hampton and Lee 1996; Masson et al. 2006). In this context, embedded

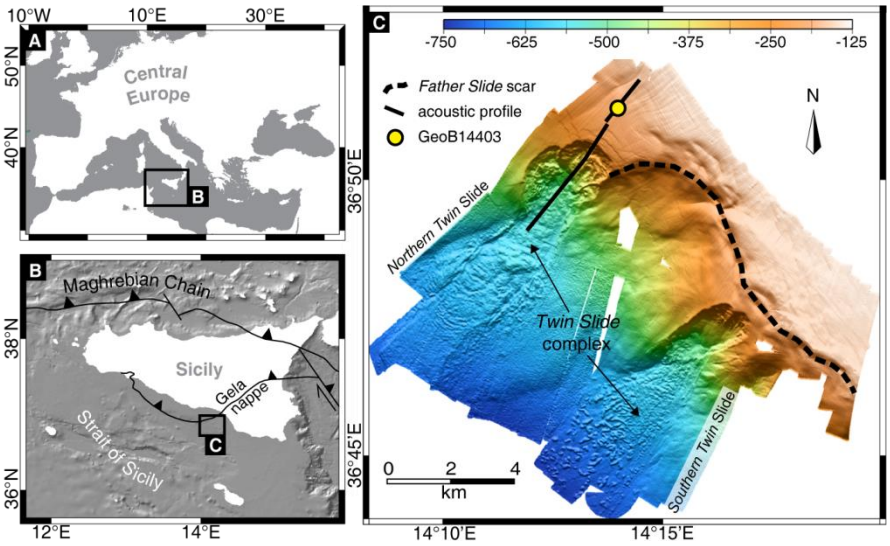

Fig. 1 a Overview of the study area in the Mediterranean Sea, **b** Location of the study area within the Strait of Sicily and major regional tectonic features, **c** Multibeam shaded relief image of the NE Gela Basin illustrating the position of drill site GeoB14403 and the acoustic profile over the *Twin Slide* complex presented in Fig. 2 (see Kuhlmann et al. 2014).

volcanoclastic layers have been proposed to act as potential detachment planes promoting translational sliding, although the exact mechanisms remain speculative (e.g., Harders 2010).

The NE region of the Gela Basin within the Strait of Sicily, Mediterranean Sea, features a continental slope that is characterized by multiple failure events of predominantly translational character (Fig. 1; Minisini et al. 2007; Minisini and Trincardi 2009; Kuhlmann et al. 2014). Along with sequence-stratigraphic boundaries, sub-horizontal volcanoclastic layers have been hypothesized as key stratigraphic surfaces that act as preferential planes of failure in this homogeneous muddy shelf-edge setting (Minisini et al. 2007; Kuhlmann et al., unpublished data). Drilled core samples from one such layer provide an excellent opportunity to test this hypothesis by evaluating the internal structure and mechanical behaviour of the volcanoclastic material and neighbouring sediment.

This study presents new evidence from geochemically identified marine marker tephra Y-7 (Kuhlmann et al. 2015), recovered at site GeoB14403 from undisturbed sediments upslope of the *Twin Slide* complex in the Gela Basin (Fig. 1c). We introduce high resolution computer tomography (CT) scans as well as drained direct-shear laboratory tests from a 20 cm whole-round (WR) core sample (GeoB14403-8 5P-2 WR) from the lithologic transition from overlying homogeneous silty clay to volcanoclastic material at a depth of ~28.2 mbsf. Additional information is provided by petrophysical Multi-Sensor Core Logger (MSCL) and geochemical X-Ray Fluorescence (XRF) data on neighbouring split core samples.

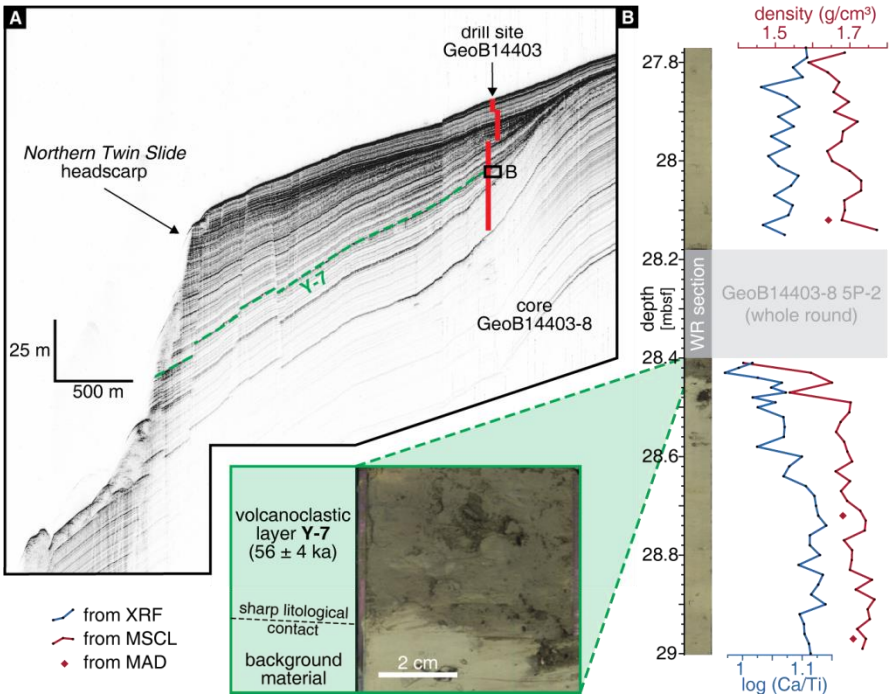

Fig. 2 a Parasound profile over the headscarp of Northern Twin Slide indicating the position of drill site GeoB14403 in the undisturbed source sediments. Volcanoclastic layer Y-7 can be traced as part of a sub-horizontal set of acoustic reflectors, **b** Investigated core section from a depth of ~27.8 – 29.0 mbsf illustrating the position of Y-7 and whole-round section GeoB14403-8 5P-2. Petrophysical and geochemical measurements indicate a significant drop in sediment density and a relative enrichment of Ti for the volcanoclastic layer compared to the background material.

2 Material and Methods

The principal data set for this study is based on a 54.6-m-long sediment succession at site GeoB14403, recovered with the Bremen seafloor drill rig MeBo (Freudenthal and Wefer 2007, 2013) during RV Maria S. Merian cruise MSM15/3 in 2010 (Fig. 2a; Kuhlmann et al. 2014; Kuhlmann et al. 2015). Acoustic data was obtained from a parametric sediment echosounder with dm-scale vertical resolution operating at 4 kHz (Atlas Parasound) and two bathymetric multibeam echosounder operating at 12 kHz (Kongsberg Simrad EM120) and 95 kHz (EM1002).

Non-destructive measurements of core-physical properties on split core sections surrounding the analysed WR section (Fig. 2b) were obtained with a GEOTEK Ltd. Multi-Sensor Core Logger (MSCL), while geochemical logging for light elements (Al to Fe) was performed with an Avaatech II core scanner using a generator setting of 10 kV, 0.2 mA and a sampling time of 20 s.

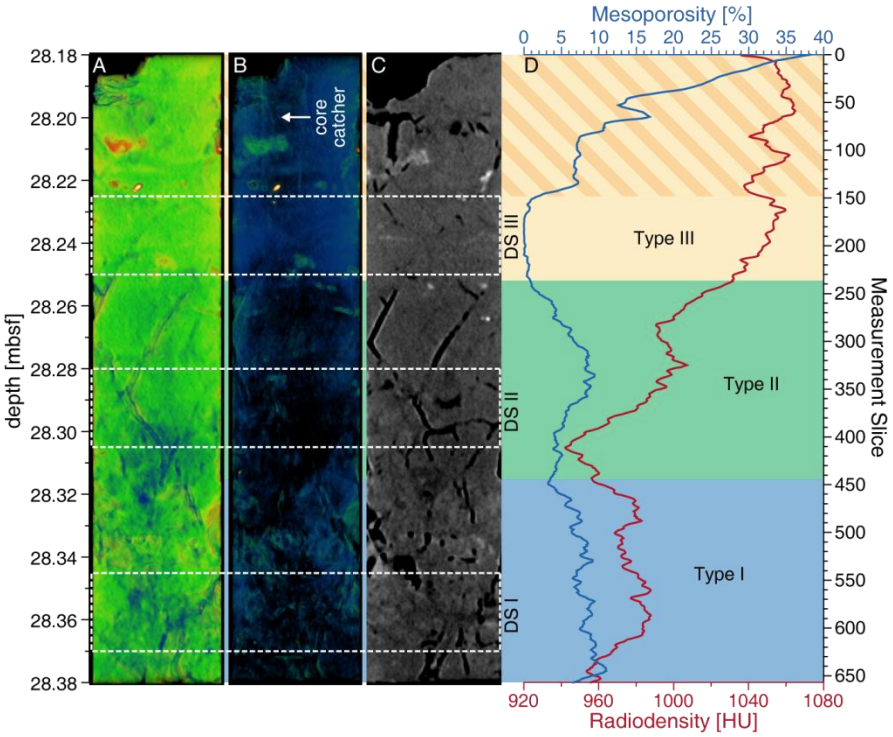

Fig. 3 Processed images and extracted information from CT data of GeoB14403-8 5P-2 WR, **a** Sliced volume image cut along depth-axis (blue colours indicate low relative density, green colours high relative density; orange/red colours show presence of very high density (i.e., shell fragments), **b** Full volume image (black/blue/green = low/high/very high relative density), **c** Thin orthoslice revealing mesoporosity, **d** Radiodensity and fraction of mesoporosity.

The 20 cm WR section GeoB14403-8 5P-2 was scanned by a Toshiba Aquilion 64 computer tomograph at the hospital Klinikum Bremen-Mitte with an exposure time of 35 s per rotation (~14 s per scan) at an X-ray source voltage of 120 kV and a tube current of 600 mA per rotation / 210 mAs. Scan resolution was 0.35 mm in x-y direction and 0.5 mm in z direction and images were reconstructed at a 0.3 mm interval. The resulting X-ray attenuation data (radiodensity) was quantified according to the Hounsfield scale (HU = Hounsfield units (Hounsfield 1973)) in order to visualize local differences in sediment densities and to extract measurements of mesoporosity (i.e., fractures; Fig. 3).

Drained direct-shear experiments on three intact samples were performed on cylindrical WR samples of 56 mm diameter and ~25 mm height using a GIESA RS5 device (see Ikari and Kopf 2011 for details). The effective normal stress (σ'_n) applied to the experiments was controlled at a constant 192 kPa to match the in situ effective vertical stress (σ'_v) at ~28 mbsf, which was calculated from shipboard bulk density measurements (Ai et al. 2014). The shear displacement for

each experiment was 12 mm, at a constant displacement rate of 0.008 mm/min to allow sample drainage and complete pore pressure dissipation (in accordance with DIN 18137-3 (Deutsches Institut für Normung 2002) and following plasticity indices presented by Ai et al. (2014)). During the test, shear stress (τ) as well as vertical and horizontal displacement were constantly measured at a frequency of 0.1 Hz.

In this study we also report an apparent coefficient of friction (μ_a) that is calculated from the effective normal stress and the measured shear stress, which includes both frictional and cohesive strengths:

$$\mu_a = \frac{\tau}{\sigma'_n} \quad (1)$$

3. Material characteristics and internal structure

The investigated depth interval exhibits a homogeneous background sedimentary section with a dominant lithology of nannofossil silty clay (Fig. 2b) (Kuhlmann et al. 2014). Shipboard moisture and density (MAD) and MSCL density values average ~1.7 g/cm³ and XRF scans reveal logarithmic Ca/Ti ratios well over the value of 1. At 28.45 mbsf the base of tephra layer Y-7 intercalates this succession, visually distinguishable by its relatively darker colour indicating increased presence of volcanoclastic material. The sharp lower contact of this layer is reflected in both physical and chemical properties, which show that density values and logarithmic Ca/Ti ratios drop significantly. The latter indicates a relative enrichment of Ti, a characteristic element in this volcanoclastic layer.

The WR section samples the upper part of Y-7 and its diffuse transition into the background material, as observed in the CT data (Fig. 3). Variability of radiodensities as well as internal fractures within this sample are observable by colour-coded reproductions of: (A) a sliced volume cut along the depth-axis, (B) the full volume data, and (C) a thin orthoslice (for information on the colour scheme please refer to the according figure legend). Additional information as to the mesoporosity (i.e., fractures) as well as the mean radiodensity within a single measurement slice (0.3 mm vertical resolution) is presented in Fig. 3d. Generally, the WR section may be subdivided into three sediment domains, each of which was sampled for subsequent direct-shear laboratory experiments as listed below (Fig. 3d):

DS I — upper section of volcanoclastic layer Y-7
(low relative radiodensity – high degree of mesoporosity)

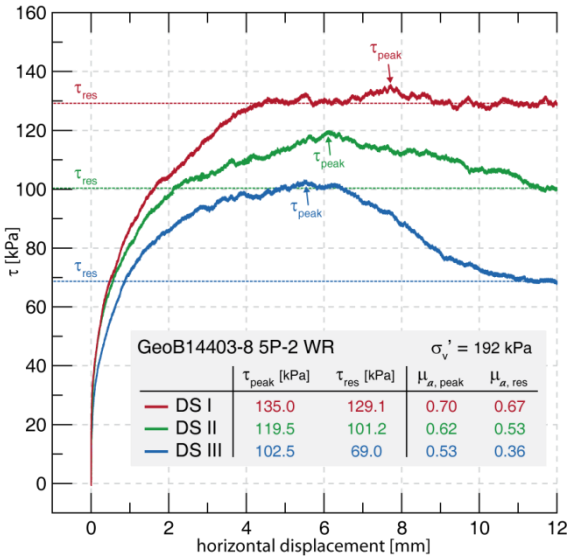

Fig. 4 Stress-strain diagram from drained direct shear experiments on samples from each sediment type of the WR section. Additionally, peak and residual values for shear strength and apparent coefficient of friction are reported. The data reveals a strain-softening behaviour of the background sediment (DS III) and significantly higher strength of the volcanoclastic layer (DS I).

DS II transitional zone
(upwards decreasing mesoporosity – respective rise in radiodensity)

DS III background material
(highest relative radiodensity – virtually no mesoporosity)

The CT data confirms the negative density anomaly of the volcanoclastic layer compared to the background material and reveals a significantly higher degree of fracturing in this layer. Note that the mesoporosity values for the upper ~4 cm of the WR section are unreliable, as they are biased by the cylindrical void left by the core catcher (Fig. 3b).

4. Drained shear strength

The experiments performed at in situ effective normal stresses reveal markedly different stress-strain behaviour for the investigated materials (Fig. 4). For the background sediment (DS III) a pronounced peak in shear strength (τ_{peak} = 102.5 kPa) followed by a decay toward a lower residual value (τ_{res} = 69.0 kPa) can be observed. In contrast, the volcanoclastic layer (DS I) maintains a relatively constant shear strength once a maximum of τ_{peak} = 135.0 kPa is reached and only slightly decreases toward a steady-state value of τ_{res} = 129.1 kPa. The stress-strain curve of sample DS II exhibits a peak strength intermediate to DS I and DS III (τ_{peak} = 119.5 kPa), but with a displacement-weakening trend similar to DS III. However, since this decay does not reach a steady value by the end of the experiment (~12 mm displacement), the residual value of τ_{res} = 101.2 kPA should be considered an upper estimate.

Correspondingly, the calculated apparent coefficients of friction (eq. 1) are lowest in case of the background material (DS III, $\mu_{peak} = 0.53$ and $\mu_{res} = 0.36$), reflecting the predominantly clayey nature of the sediment. With increasing volcanoclastic content these increase to a maximum of $\mu_{peak} = 0.7$ and $\mu_{res} = 0.67$ in sample DS I.

5. Discussion and Conclusions

The investigated core interval, which samples the transition from homogeneous background sediments to marine marker tephra Y-7, reveals fundamental differences between the two end members in terms of internal structure and shear strength and suggests that failure would require two distinct failure mechanisms.

The background sediment displays the lowest peak shear strength of all three investigated samples under drained conditions and may be considered as the most susceptible to failure. It follows a stress-strain path indicating strain-softening behaviour typical for the reorientation of clay particles parallel to the direction of shear – a characteristic that favours the phenomenon of progressive failure and hence the development of failure surfaces once shear stresses locally reach the material peak strength (e.g., Leroueil 2001). This material behaviour is absent within the ash-bearing layer and appears to correlate with diminished volcanoclastic content.

While mechanical investigations provide evidence of preferential failure within the background material, mesoscale observations suggest a distinct failure mechanism that relates to the volcanoclastic layer, which works on much shorter timescales: excess pore pressure generation in response to external transient events. Existing fractures within the volcanoclastic layer may host significant volumes of fluid, which could generate transiently elevated pressures in response to temporarily undrained conditions. In order for the volcanoclastic layer to act as a failure plane it must become weaker than the surrounding silty clay. Assuming a constant apparent coefficient of friction, this would require a reduction in effective normal stress via an increase in pore water pressure of ≥ 45.6 kPa for domain DSI (eq. 1). With diminished volcanoclastic content this value decreases to ≥ 26.7 kPa for domain DSII and approaches 0 near the volcanoclastic/silty clay boundary, suggesting preferential failure along this interface. This mechanism is similar to the weak layer generation through rearrangement of ash-particles as previously proposed by Harders et al. (2010), though it works on a different spatial scale.

Considering the high frequency of failure, we propose a seismic trigger (see Minisini et al. 2007; Ai et al. 2014) to repeatedly invoke the above introduced mechanism. We suggest that transiently increased fluid pressures due to earthquake shaking may promote instantaneous translational sliding along the interface between embedded volcanoclastic material and overlying regular sediments – thus impeding failure initiation within the background sediments, which are weaker

over longer timescales. Evidence of volcanoclastic layers at the base of two drilled mass-transport deposits further supports this theory (Kuhlmann et al., unpublished data). In the framework of submarine slope stability in muddy shelf-edge settings, our results indicate that given the occurrence of suitable transient external events (i.e., earthquakes) at the site of investigation, slope failure depends on a competition between mechanical sediment properties and hydrologic effects via mesoscale structures such as fracturing, as frequently found in marine volcanoclastic layers.

Acknowledgments This work has been funded by the DFG through MARUM – Universität Bremen. We gratefully acknowledge the constructive reviews by Dr. Marzia Rovere and Dr. Rieka Harders and wish to particularly thank Dr. Gauvain Wiemer for his help with the shear box experiments as well as Dr. Jürgen Titschack for support with the CT data. MSCL and XRF core scanning were carried out at the lab facilities of MARUM.

References

Ai F, Kuhlmann J, Huhn K et al (2014) Submarine slope stability assessment of the central Mediterranean continental margin: the Gela Basin. In: Krastel S, Behrmann J-H, Völker D et al (eds) Submarine Mass Movements and their Consequences. Springer, Heidelberg, pp 225-236

Deutsches Institut für Normung (2002) Soil, investigation and testing – Determination of shear strength – Part 3: Direct shear test. Rep DIN 18137-3, Berlin

Freudenthal T, Wefer G (2007) Scientific drilling with the sea floor drill rig MeBo. doi: 10.5194/sd-5-63-2007

Freudenthal T, Wefer G (2013) Drilling cores on the sea floor with the remote-controlled sea floor drilling rig MeBo. doi: 10.5194/gi-2-329-2013

Hampton MA, Lee HJ (1996) Submarine landslides. doi: 10.1029/96RG03287

Harders R, Kutterolf S, Hensen C (2010) Tephra layers: A controlling factor on submarine translational sliding? doi: 10.1029/2009GC002844

Hounsfield GN (1973) Computerized transverse axial scanning (tomography). Part I. Description of system. doi: 10.1259/0007-1285-46-552-1016

Ikari MJ, Kopf AJ (2011) Cohesive strength of clay-rich sediment. doi: 10.1029/2011GL047918

Kuhlmann J, Asioli A, Strasser M et al (2014) Integrated stratigraphic and morphological investigation of the Twin Slide complex offshore southern Sicily. In: Krastel S, Behrmann J-H, Völker D et al (eds) Submarine Mass Movements and their Consequences. Springer, Heidelberg, pp 583-594.

Kuhlmann J, Asioli A, Trincardi F et al (2015) Sedimentary response to Milankovitch-type climatic oscillations and formation of sediment undulations: evidence from a shallow-shelf setting at Gela Basin on the Sicilian continental margin. doi: 10.1016/j.quascirev.2014.10.030

Leroueil S (2001) Natural slopes and cuts: movement and failure mechanisms. doi: 10.1680/geot.2001.51.3.197

Masson DG, Harbitz CB, Wynn RB et al (2006) Submarine landslides: processes, triggers and hazard prediction. doi: 10-1098/rsta.2006.1810

Minisini D, Trincardi F, Asioli A et al (2007) Morphologic variability of exposed mass-transport deposits on the eastern slope of Gela Basin (Sicily channel). doi: 10.1111/j.1365-2117.2007.00324.x

Minisini D, Trincardi F (2009) Frequent failure of the continental slope: The Gela Basin (Sicily Channel). doi: 10.1029/2008JF001037